

HYDROTHERMAL MANGANESE DIOXIDE: SYNTHESIS, STRUCTURE, MORPHOLOGY AND DISCHARGE PERFORMANCE

by
Daud K. Walanda, Geoffrey A. Lawrance and
Scott W. Donne*

Discipline of Chemistry
University of Newcastle
Callaghan, NSW 2308
AUSTRALIA

ABSTRACT

Digestion of Mn_2O_3 in a range of H_2SO_4 solutions (0.01-10.0 M), at a variety of temperatures (20°-140°C) has led to the formation of a series of kinetically stable manganese dioxide samples via a dissolution-precipitation mechanism involving disproportionation of a soluble Mn(III) intermediate. The resultant manganese dioxide samples were characterized in terms of their domain of phase stability, chemical composition, structure, morphology and electrochemical performance. $\gamma\text{-MnO}_2$ predominated at all but high H_2SO_4 concentrations (>5 M), where $\alpha\text{-MnO}_2$ was formed, and high temperatures (>80°C) where $\beta\text{-MnO}_2$ was formed, as shown in Figure 1.

The structural variety of $\gamma\text{-MnO}_2$ in its domain of stability was interpreted in terms of the fraction of De Wolff defects (P_r), which was found to increase as the H_2SO_4 concentration was decreased and the temperature was increased, microtwinning (T_w), which despite being less statistically significant, was found to follow a similar trend, and cation vacancy fraction and Mn(III) fraction. Both the latter structural properties decreased as the temperature was increased; however, decreasing the H_2SO_4 concentration led to a decrease in cation vacancy fraction but an increase in Mn(III) fraction. These structural characteristics, in particular De Wolff defects, were interpreted on a molecular level in terms of soluble Mn(III) intermediate condensation in which the electrolyte conditions determine the relative proportions of equatorial-axial edge sharing (ramsdellite domains only) and equatorial-axial corner sharing (both ramsdellite and pyrolusite domains) that occurs.

Morphological differentiation was easily established due to the different characteristics of each phase. $\gamma\text{-MnO}_2$ existed as fine needles (250 nm × 50 nm), $\beta\text{-MnO}_2$ was formed as much larger columns (1 μm × 100 nm), while $\alpha\text{-MnO}_2$ was present as small spheres up to 400 nm in diameter.

Electrochemical characterization by voltammetry (Figure 2) in an aqueous 9 M KOH electrolyte demonstrated that the performance of the $\gamma\text{-MnO}_2$ samples was comparable to that of commercial EMD, whereas α - and $\beta\text{-MnO}_2$ suffered from diffusional limitations which lowered their operating voltage. For $\gamma\text{-MnO}_2$, superior performance resulted when lower temperatures and H_2SO_4 concentrations were used, corresponding to intermediate levels of De Wolff defects and microtwinning, but a cation vacancy fraction minimum.

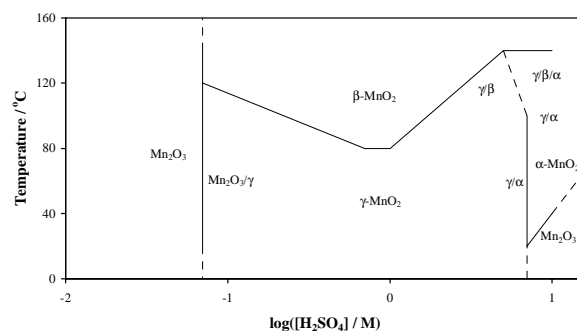


Figure 1. Phase diagram resulting from Mn_2O_3 digestion in H_2SO_4 solutions.

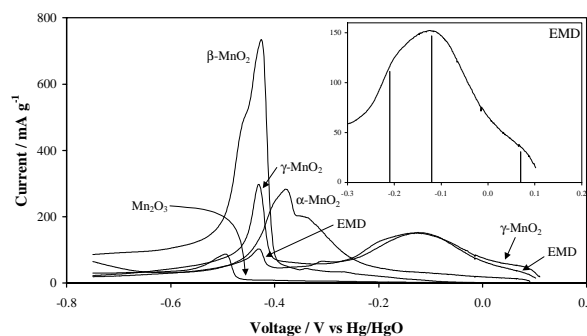


Figure 2. Representative electrochemical discharge data.